Annu. Rev. Fluid Mech. 2004. 36:29–53
doi: 10.1146/annurev.fluid.36.050802.122049

COATING FLOWS

Steven J. Weinstein and Kenneth J. Ruschak
Eastman Kodak Company, Rochester, New York 14652-3703;
email: steven.weinstein@kodak.com, kenneth.ruschak@kodak.com

Key Words liquid films, coating dies, liquid curtains, dynamic wetting, coating methods

■ **Abstract** Coating is the process of applying thin liquid layers to a substrate, often a moving web. Complex coating processes can be approached through examination of their fluid mechanical components. The flow elements reviewed in this article include the boundary layer along a moving wall, the dynamic wetting line, withdrawal from a pool, flow metered by a narrow channel, die flow, flow on an incline, the freely falling liquid curtain, premetered coating with a small gap, and flow after coating. Although some flow elements are well studied and understood, others require additional investigation. Genuinely predictive modeling of complex coating processes is not yet possible and coating practice remains largely empirical. Nonetheless, coating science is sufficiently advanced that physical insights and mathematical models greatly benefit design and practice.

INTRODUCTION

Coating is the process by which thin liquid layers are formed and applied to a solid surface. Coating flows are the flows utilized in coating processes and also include the incidental flows that occur after coating and before immobilization. This article focuses on the continuous coating of wide webs, which gives rise to ideally two-dimensional, steady laminar flows. As discussed in an earlier review by Ruschak (1985), coating processes may be broadly classified as self-metered or premetered (Figure 1). In self-metered flow, the liquid properties, web speed, and geometry combine to determine the thickness of the coated film. Self-metered methods include dip, roll, and blade coating (Figure 1*a*,*b*,*c*). In premetered coating processes, direct setting of the flow rate determines the thickness of the coated film independently of these parameters. Premetered methods require a precision liquid delivery system and a die for widthwise distribution. These methods include slot coating, slide coating, and curtain coating (Figure 1*c*,*d*,*e*).

A genuinely predictive analysis of a realistic coating process is generally not possible, and the number of coating methods is extensive. It is therefore advantageous to examine the fluid mechanical components (flow elements) comprising

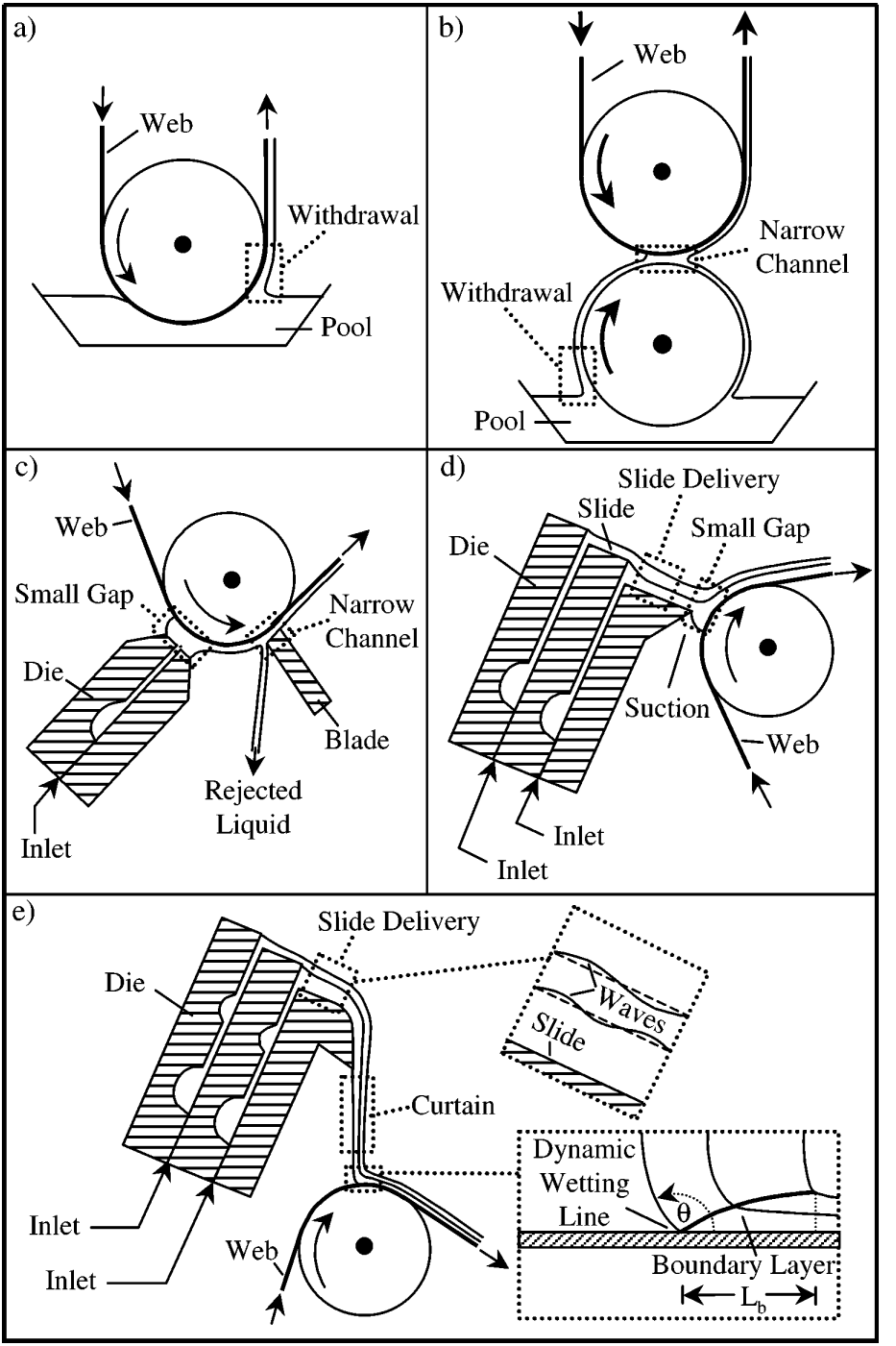
a)
Web
Withdrawal
Pool
b)
Web
Narrow
Channel
Withdrawal
Pool
c)
Web
Small Gap
Narrow
Channel
Die
Blade
Rejected
Liquid
Inlet
d)
Slide Delivery
Slide
Small Gap
Die
Suction
Web
Inlet
Inlet
e)
Slide Delivery
Die
Waves
Slide
Curtain
Dynamic
Wetting
Line
θ
Inlet
Inlet
Web
Boundary Layer
L_b

coating processes and then combine this knowledge for applications. The knowledge of interest includes achievable coating thickness and uniformity, attainable speed, rheological requirements, and tolerable levels for flow perturbations. A specific coating process may be viewed as an optimization among its component flow elements to achieve specified objectives. In this review, we examine common flow elements, many of which are illustrated in Figure 1. The flow of a thin film of gradually varying thickness, common to many elements, is considered first. The boundary layer along a moving wall affects the position of the dynamic wetting line (Figure 1*e*), which can, in turn, greatly affect dynamic wetting and coating speed. Self-metered flow elements include withdrawal from a pool, used as a direct coating method (Figure 1*a*) or a feed (Figure 1*b*). A narrow channel often serves as a metering flow element and is found in roll coating (Figure 1*b*) and blade coating (Figure 1*c*). Premetered coating methods use coating dies (Figure 1*c*,*d*,*e*) to distribute liquid widthwise to form nearly uniform sheets; their design is complicated by rheological and mechanical constraints. In the simultaneous coating of multiple layers, flow along the inclined, external surfaces of the die, called the slides (Figure 1*d*,*e*), may develop waves that can degrade coating uniformity (Figure 1*e*). Curtains, freely falling liquid sheets (Figure 1*e*), are central to the curtain coating method. Relevant issues are curtain integrity and the response of the curtain to ambient perturbations that threaten uniform coating. Another important flow element is premetered coating with a small gap and a liquid bridge or bead spanning the gap (Figure 1*c*,*d*). Of importance is the ability of the interfaces bounding the bead to bridge the gap between the coating die and the web, as this is a necessary condition for uniform coating. Immediately after coating and prior to immobilization, liquid may redistribute. Flow after coating encompasses incidental flow due to ambient perturbations, inclination of the web, and an uneven web surface.

Given the broad area encompassed by coating and limited space, our review selectively cites the literature illuminating common flow elements with emphasis on recent contributions. We present many results for shear-thinning liquids to emphasize their prevalence in coating processes. We do not examine viscoelastic liquids, which typically make the coating of a uniform layer more difficult and lack broadly applicable constitutive equations that enable generalizing results. We do not examine specific coating processes and their practical range of operation; the reader is referred to books by Kistler & Schweizer (1997), Walter (1993), and Lehtinen (2000), as well as the patent literature, for this information.

←

Figure 1 Coating methods and their flow elements. (*a*) Self-metered dip coating; (*b*) self-metered roll coating; (*c*) premetered slot coating, followed by self-metered blade coating; (*d*) premetered slide coating; (*e*) premetered curtain coating, with expanded views of a slide delivery flow with waves, the dynamic wetting line, the dynamic contact angle, θ, and the boundary layer along a moving web with length L_b.

THE FLOW OF A THIN FILM

The flow of thin films adjacent to walls is common to several flow elements, and so we address it separately. In regions of a coating process, it is often the case that film thickness changes gradually. Inertia may be neglected for small values of the modified Reynolds number, the product of the usual Reynolds number and the aspect ratio. Thus, when a small aspect ratio is imposed by walls, such as rollers and doctoring blades, classical lubrication theory applies (Cameron 1976, Dowson & Higginson 1977). By contrast, the aspect ratio is not always anticipated in a free-surface flow, and often the modified Reynolds number is not small. As a result, inertia must be included, and a boundary-layer form of the momentum equation (Levich 1962, Schlichting 1979) is required.

In general, the boundary-layer equations for thin-film flows generate formidable free-surface problems. Similarity transforms of free-surface flows are available only in special cases (Rosenhead 1940, Watson 1964, Ruschak 1974). In cases of steady flow without recirculation, the von Mises transformation can map the flow domain into a rectangular strip and give the momentum equation the form of a heat transfer equation (Schlichting 1979, Ruschak & Weinstein 2001). Aside from these special cases, more direct numerical techniques must be employed.

The von Kármán-Polhausen method offers a simplified approach to solving boundary-layer equations approximately. An assumed velocity profile is inserted into an integral form of the momentum equation (Schlichting 1979). The result is a nonlinear ordinary differential equation for the film thickness (Kheshgi et al. 1992) that we refer to as a film equation. This averaging approach is practical because predictions of the film equation are often not sensitive to the assumed velocity profiles (Andersson 1987). A natural choice for the velocity profile for Newtonian flow is a half-parabola, as this is the exact profile for fully developed flow on a flat wall. Furthermore, when inertia is negligible, steady film equations reduce to those obtained by lubrication theory (Levich 1962) for which a parabolic profile is asymptotically correct. When predicted interface shapes have small slopes, film equations generally lead to results accurate enough for most purposes (Kheshgi 1989, Ruschak & Weinstein 2003).

We now consider a film equation valid for a power-law liquid on a flat wall moving at speed S in the direction x at an angle θ to the horizontal, where $0 < \theta < \pi$ indicates motion against gravity, g. The location of the air-liquid interface is represented as $y = h(x)$, where y measures the distance across the film, x is the distance along the wall, and the limiting film thickness downstream is h_∞. The viscosity of the liquid is expressed as $\eta = m\gamma^{n-1}$, where m is the consistency, n is the power-law exponent, and γ is the magnitude of the rate of strain. The liquid has density, ρ, and the air/liquid interface has surface tension, σ. A velocity field, v_x, that is consistent with the fully developed flow downstream and reduces to a parabolic profile for the Newtonian case ($n = 1$), is

$$v_x = \frac{(1+2n)}{(1+n)} \frac{(q - Sh)}{h} \left[1 - \left(1 - \frac{y}{h} \right)^{1+1/n} \right] + S, \tag{1}$$

where q is the volumetric flow rate per unit width. Inserting Equation 1 into the integral form of the momentum equations simplified for small slope, we obtain the following film equation:

$$\rho(ah^2S^2 - bq^2 + gh^3\cos\theta)\frac{dh}{dx} = -\rho gh^3\sin\theta - cmh^{2-2n}(q - Sh)|q - Sh|^{n-1} + \sigma h^3\frac{\partial\kappa}{\partial x} \tag{2a}$$

$$\kappa = \frac{\partial^2 h}{\partial x^2}, \quad a = \frac{n}{(2+3n)}, \quad b = \frac{2(1+2n)}{(2+3\dot{n})}, \quad c = \left(\frac{1+2n}{n}\right)^n. \tag{2b}$$

With $\eta^* = m(S/h_\infty)^n$ as a characteristic viscosity of the liquid, the dimensionless groups that arise are the Reynolds number, $Re = \rho Sh_\infty/\eta^*$, the capillary number, $Ca = \eta^* S/\sigma$, and the gravitational number, $\beta = \rho g{h_\infty}^2/\eta^* S$. In practice, the film Equation 2 applies for large surface tension ($Ca \ll 1$) or large inertia ($Re \gg 1$); creeping flows with $Ca \gg 1$ typically have large slopes and the film equations fail. The aspect ratio ε of the film can be related to either Re or Ca, depending on whether surface tension or inertia dominates.

As $Ca \to 0$, the aspect ratio is $\varepsilon = Ca^{1/3}$, and all gravitational and inertial terms are lost from the film equation. For film formation in this case, the film equation connects to an effectively static meniscus upstream that has a radius of curvature, R, at the location where the meniscus appears to be tangent to the moving wall. A relationship between h_∞ and R is given by

$$h_\infty = [K(n)R]^{3/(2n+1)}\left[\frac{mS^n}{\sigma}\right]^{2/(1+2n)}, \quad K(n) = 2.553e^{-0.65n}, \tag{3}$$

consistent with the result of Gutfinger & Tallmadge (1965); the empirical function K in Equation 3 has been fitted to numerical results. The Newtonian counterpart of Equation 3 is the classical Landau-Levich equation (Levich 1962), which follows from Equation 3 when $n = 1$ ($K = 1.34$), and $m = \mu$, where μ is the viscosity. Equation 3 indicates that reducing R by confining the meniscus between closely spaced walls leads to thinner coatings. Low-speed coating processes can be viewed as different ways to control meniscus curvature.

Experiments for Newtonian liquids indicate that Equation 3 is valid for $Ca < 0.01$. In computations, using the complete expression for curvature, κ, instead of the linearized approximation in Equation 2, provides a smooth transition to the nearly hydrostatic region as $h \to \infty$. Although the original boundary-layer system neglects $O(\varepsilon^2)$ terms, suggesting a linearized form for κ as given in Equation 2b, this approach retains terms that are essential to either the thin-film region or the static region to obtain a composite equation accommodating both regions. The composite equation is effective, provided that the dynamic terms become small while the slope of the interface is small, i.e., before the static region is reached. An alternative is to solve a singular perturbation problem that is often formidable (Ruschak 1974, Wilson 1982) and more limited in range. The approach of retaining

terms in film equations significant in different regions of flow, even when not uniformly asymptotically justified, has successfully predicted complete interface profiles in a variety of configurations (Ruschak 1978, Kheshgi et. al. 1992, Ruschak & Weinstein 1999).

At $Re \gg 1$, the aspect ratio of the film is $\varepsilon = 1/Re$, and the surface-tension term in Equation 2a is of order $1/(Re^3Ca)$. As a result, Equation 2a reduces to a first-order nonlinear equation of the form $dh/dx = N(h)/D(h)$. Film equations of this form can exhibit a singularity where $D(h) = 0$, called a critical point. Examining wave motion reveals a second-order hyperbolic structure, and $D(h) = 0$ corresponds to a transition from subcritical (waves can move in the upstream and downstream directions) to supercritical (waves move downstream only) flow (Weinstein & Ruschak 2001). In circumstances where a film thins in the direction of flow and changes from subcritical to supercritical, $N(h)$ can be adjusted to eliminate the singularity at $D(h) = 0$ by choice of film thickness at the critical point. In this case, the critical point has both an upstream and downstream influence on the film profile. The resulting solution for $h(x)$ is continuous at all orders. Such structures occur in dip-coating flows (Cerro & Scriven 1980, Weinstein & Ruschak 2001), weir flows (Ruschak & Weinstein 1999), and open-channel flows (Dressler 1949). They also arise in inviscid curtain flows, but these involve surface tension (Finnicum et al. 1993, Weinstein et al. 1997).

In configurations where the film thickens in the direction of flow and $D(h) = 0$ in the flow domain, a film equation using a self-similar velocity profile (i.e., a profile of fixed shape but variable magnitude), such as Equation 1, fails. The critical point cannot exert an influence on the upstream supercritical region, and $N(h)$ cannot be adjusted to eliminate the singularity. Under such circumstances, a higher-order velocity profile, such as a third-order polynomial in the case of a Newtonian liquid, must be employed (Bohr et al. 1997, Ruschak & Weinstein 2001). A more general profile adds dispersive behavior to the wave equation and enables limited upstream influence of the critical point. Although the limit of negligible surface tension removes the highest derivative in Equation 2, the resulting solution is uniformly valid even in the vicinity of the critical point (Weinstein & Ruschak 1999).

THE BOUNDARY LAYER ALONG A MOVING WALL

Laminar boundary layers arise from the entrainment of air or liquid by a moving wall and influence the operating ranges of coating processes. These boundary layers are different from those arising in the classical theory (Schlichting 1979) along stationary or moving plates with a leading edge and are called Sakiadis boundary layers (Sakiadis 1961a,b). Although the boundary-layer equation is the same as in the classical case, the boundary conditions differ. In coating processes, boundary layers in the liquid start at the dynamic wetting line and grow along the web (Figure 1*e*). An air boundary layer can disturb the coating process where the air is displaced by the liquid in the vicinity of the dynamic wetting line. We focus here on an important length, the distance from the wetting line to where all

metered liquid is entrained and the film begins to relax toward its final thickness. A von Kármán-Polhausen approximation can be used to estimate this length.

Fox et al. (1969) performed such an analysis for a power-law liquid using for the velocity profile a piecewise fourth-order polynomial tending to zero far from the wall. Here we consider that the velocity far from the wall, S_∞, is not zero, and generalize the analysis of Blake et al. (1994) using a velocity profile of the form

$$v_x = (S_\infty - S)\left[1 - \left(1 - \frac{y}{\delta(x)}\right)^{1+1/n}\right] + S, y \le \delta(x); \quad v_x = S_\infty, y > \delta(x), \tag{4}$$

where $\delta(x)$ is the boundary layer thickness. Inserting this profile into the integral boundary layer equation yields an expression for the boundary-layer length, L_b, (Figure 1*e*):

$$\frac{L_b S}{q} = \left(\frac{n(1+2n)}{(1+n)(n+(n+1)\varphi)}\right)^{n+1}\left(\frac{1+2n+(1+n)\varphi}{(2+3n)(1+2n)(1-\varphi)^{n-1}}\right) \times \left(\frac{\rho q^n}{m S^{2n-2}}\right), \quad \varphi = \frac{S_\infty}{S}. \tag{5}$$

The result of Blake et al. (1994) is recovered in the Newtonian limit.

The velocity profiles obtained by numerically solving the Sakiadis boundary layer equations have been experimentally verified under both laminar and turbulent conditions for Newtonian liquids (Tsou et al. 1967). The stability of the Newtonian Sakiadis boundary layer has been examined by a classical Orr-Sommerfeld analysis (Tsou et al. 1966). The Sakiadis boundary layer is more stable than its conventional Blasius counterpart, and its small length in typical coating flows assures stability.

THE DYNAMIC WETTING LINE

Dynamic wetting is central to the coating process primarily because coating speed is limited by a maximum speed of wetting and air entrainment (Kistler & Schweizer 1997). Nonetheless, its physics is still debated, and genuinely predictive models remain elusive. The classical equations of hydrodynamics have no solution if a dynamic wetting line (Figure 1*e*) is present. Ostensibly, a contact angle (i.e., θ in Figure 1*e*) has to be supplied as a boundary condition as part of a well-posed equation set just as in capillary statics. However, experiments show that the observable contact angle varies with material properties, speed, and in general the details of the flow field. It is not surprising that most coating-flow simulations circumvent the issue.

Hansen & Toong (1971) first proposed that the contact angle is the static-advancing contact angle and that hydrodynamic bending of the interface at microscopic distances from the wetting line gives rise to the visible speed-dependent

contact angle. A well-posed set of equations is usually obtained by replacing the no-slip boundary condition at the wall with a slip condition, often the Navier condition that slip is proportional to shear stress. Asymptotic formulas relating the actual and observable contact angles are available over the entire range of Reynolds numbers for a Newtonian liquid for capillary numbers less than about 0.1 and for a slip length that is small compared to the characteristic flow dimension (Cox 1998). What sets the slip length is not definite, but the hydrodynamic bending and the observable contact angle increase as slip length decreases. Often, the slip length is determined by fitting contact-angle data. However, Shen & Ruth (1998) fit the model to their measurements of meniscus shape in the range of 5–200 microns from the wetting line, and they found that the speed dependence of the contact angle was largely attributable to variation of the actual angle. Voinov (1994) extended hydrodynamic theory to a shear-thinning liquid by estimating a local shear rate and apparent Newtonian viscosity.

Molecular kinetic theory treats the dynamic contact angle as an irreversible rate process. Inherent in this approach is the view that the observable contact angle is the actual contact angle and that it varies with speed. The theory supplies a contact angle but does not directly lead to well-posed hydrodynamics. Recently, this model was extended to take specific account of solid-liquid interactions (Blake & De Coninck 2002). The modified theory can account for experimental results showing that the maximum speed of wetting attains a maximum value at some intermediate value of the static contact angle. Increasingly sophisticated simulations of molecular dynamics provide strong support for molecular-kinetic theory (de Ruijter et al. 1999).

Shikhmurzaev (1996, 1997) proposed a substantial alteration of the classical boundary conditions of hydrodynamics that conceptually is a middle ground between the hydrodynamic and molecular kinetics approaches. The interfaces are considered to be thin fluid phases with equations of state relating, in the simplest case, surface pressure to surface mass density. The liquid-air interface moves through the wetting line to the liquid-solid interface, and its properties change to new equilibrium values over a relaxation time. The relaxation process leads to gradients in surface pressure that cause shearing of the interfaces and apparent slip of the bulk liquid at the wall. The resulting boundary condition is the Navier slip condition augmented with a term for the surface pressure gradient. Additionally, a force balance at the wetting line leads to a dynamic Young's equation and a speed-dependent dynamic contact angle because of the departure of the surface pressures from their equilibrium values. An attractive feature of this model is that interface formation gives rise to both apparent slip and a speed-dependent contact angle. A clear disadvantage is the large number of physical parameters required to model the interfaces even in the simplest case. The lack of information about these parameters does not allow direct comparison with experiments, but data for the dynamic contact angle can be represented using plausible values (Blake & Shikhmurzaev 2002).

For macroscopic flows at low *Ca*, there is experimentally a maximum speed of wetting that is independent of the hydrodynamics (Petrov & Sedev 1985, Cohu &

Benkreira 1998a, Benkreira & Cohu 1998). The relevant wetting-line speed is the component of the wall speed normal to the wetting line. When wall speed exceeds the maximum speed, the wetting line breaks into straight segments that are angled to the wall velocity such that the maximum speed is not exceeded. Cylindrical air tubes extending in the direction of wall velocity may develop at downstream vertices, and these may break into air bubbles through surface tension–driven instability (Simpkins & Kuck 2000). The maximum speed increases with increasing surface tension and decreasing viscosity. For shear-thinning liquids, the apparent viscosity is relevant, although the applicable shear rate is not definite (Ghannam & Esmail 1997, Cohu & Benkreira 1998b).

Practitioners of the coating art know that the air-entrainment speed depends not only on the materials but also on the coating method and its parameters, but documentation of this knowledge in scientific literature has been scant. Some results are available for curtain coating, where parameters including the flow rate, curtain impingement speed, and angle influence the dynamic contact angle and the air entrainment speed (Blake et al. 1994, Blake et al. 1999, Clarke 2002). For example, air-entrainment speed increases roughly linearly with impingement speed, and the term hydrodynamic assist was introduced to emphasize that the flow can be manipulated to increase speed. Wilson et al. (1999) showed that the hydrodynamic model with invariant actual contact angle cannot account for this data. Blake et al. (1994) showed that the highest speeds correspond to a wetting-line position directly beneath the curtain. More specifically, the distance of the wetting line from the downstream surface of the curtain divided by the projected width of the curtain on the moving wall, termed the relative wetting-line position, is optimally about 0.7. The relative wetting-line position may be computed from the boundary-layer length, $L_{b,}$ given by Equation 5. The relative wetting-line position can account for why, contrary to expectations from experiments with solid surfaces plunging into liquids, air-entrainment speed may not increase in curtain coating when viscosity is lowered. Clarke (2002) also reported a synergy involving high viscosity, high impingement speed, and average peak-to-peak wall roughness, R_z, in the range 2–12 microns. To influence dynamic wetting, the flow must presumably be altered on a length scale comparable to that of the region near the wetting line where nonclassical hydrodynamics operates, and so the small scale of the impingement zone in curtain coating, about 100 microns, may be crucial. For models of dynamic wetting to be generally applicable, the customary restrictions to small capillary number and to flows with a characteristic dimension much larger than the region of nonclassical slip hydrodynamics may have to be dropped.

SELF-METERED FLOW ELEMENTS

Withdrawal from a Pool

Withdrawal from a pool is used to form coatings directly as in dip coating (Figure 1*a*) or to supply liquid to a downstream element as in roll coating

(Figure 1*b*). Kistler & Schweizer (1997) review the dip coating of flat surfaces, primarily for Newtonian liquids.

At small capillary number, Equation 3 applies to dip coating. The radius of curvature of the interface, R, is determined by the essentially static meniscus as it approaches the moving wall, and the thickness of the entrained film from a large pool follows as (Levich 1962, Gutfinger & Tallmadge 1965)

$$h_\infty = \left[\frac{\sigma K(n)^2}{2\rho g(1-\cos\theta)}\right]^{3/(4n+2)} \left(\frac{mS^n}{\sigma}\right)^{2/(1+2n)}, \tag{6}$$

where the notation is defined above. Films thinner than that given by Equation 6 may be achieved by reducing the radius of curvature of the meniscus by obstructing the pool (Deryagin & Levi 1964, Kheshgi et al. 1992).

The Newtonian case of Equation 6 has been verified in many experiments (Groenveld 1970, Kitzio et al. 1999), which indicate the range $Ca \leq .01$ when inertia is negligible. Conversely, experimental results have not agreed with the general power-law result, Equation 6, that overpredicts coating thicknesses (for a review, see Dutta & Mashelkar 1982). The cause of this disparity has yet to be determined but does not appear to be a deficiency of the power-law constitutive equation at low shear (Hildebrand & Tallmadge 1968, Spiers et al. 1975).

Under conditions of moderate Re but low Ca, film equations may be used to couple the viscous film region with a static meniscus (Keshgi et al. 1992) as discussed above. However, when $1/(Re^3Ca) \ll 1$, surface tension effects are negligible, and a critical point arises in the film Equation 2. Removing this singularity sets the volumetric flow rate in the film and therefore determines the final film thickness, h_∞. For the case of vertical withdrawal ($\theta = \pi/2$), the volumetric flow rate is given by

$$q = \left[\frac{e^{1/2}-1}{2e^{1/(2n)}}\right]^{n/(n+1)} \left(\frac{mS^{2n+1}}{\rho g}\right)^{1/(n+1)}, \quad e = \frac{2(1+2n)}{n}, \tag{7a}$$

and h_∞ is the asymptotic solution of Equation 2

$$h_\infty = C(n)\left(\frac{mS^n}{\rho g}\right)^{1/(1+n)}, \quad C(n) = \frac{1.39n^{.63}}{1+1.22n^{.63}}, \tag{7b}$$

where $C(n)$ is an empirical representation of numerical results. Cerro & Scriven (1980) derived Equation 7b for the vertical withdrawal of a Newtonian liquid with $C = 0.63$. Extensive experimentation for vertical withdrawal yields $C = 0.67 \pm 0.02$ (for example, Van Rossum 1958, Groenveld 1970, Kitzio et al. 1999), but there are no results for shear-thinning liquids. Weinstein & Ruschak (2001) generalized Equation 7 for a nonvertical web for a Newtonian liquid but, again, there are no experimental results for comparison.

The low Ca and high Re limits discussed above provide asymptotes to the experimental film thickness data for Newtonian liquids for the case of vertical withdrawal (Kitzio et al. 1999). Numerical solution of the complete equation set is required to predict h_∞ under intermediate conditions (Reglat et al. 1993).

Narrow Channel

In coating methods including roll (Figure 1*b*) and blade coating (Figure 1*c*), narrow channels are employed to form a liquid layer and control its thickness. The thickness of the coated film is comparable to the minimum gap, and consequently tight mechanical tolerances are required to create a thin film. A precision gap may be set, but the thinnest films result when one wall is pressed against the other with hydrodynamic forces maintaining a slight separation (Cohu & Magnin 1997, Carvalho & Scriven 1997). In this latter case, at least one of the channel walls must be a compliant member, such as an elastomer-covered roller or a flexible blade. Kistler & Schweizer (1997) and Lehtinen (2000) provide reviews of roll and blade coating.

The flow in a slowly varying channel can be analyzed using the lubrication approximation. Usually there is a boundary condition on pressure at each end to determine the pressure level and flow rate. When a film-forming meniscus is present, an additional boundary condition is required to determine its position, namely the pressure gradient in the lubrication flow at the meniscus. This pressure gradient is also crucial to the ribbing instability discussed below. The difficulty inherent in using the lubrication approximation is providing this boundary condition because the lubrication flow in the channel does not determine the meniscus position or how the flow divides in the case of two films (Gaskell et al. 1998a). The boundary conditions can be determined by analyzing the two-dimensional flow in the proximity of the meniscus considering the channel walls parallel (Ruschak 1982, Coyle et al. 1986) or diverging (Halpern & Jensen 2002). However, at small capillary number, the required boundary conditions can be derived from the Landau-Levich film-forming Equation 3 (Ruschak 1991, Gaskell et al. 2001). In this situation, surface tension dominates the shape of the central portion of the meniscus, and the influence of the two-dimensional flow away from the film-forming zones adjacent to the walls is inconsequential.

Forward roll coating is used to coat films directly or to feed a subsequent metering element such as a blade. The channel walls move in the same direction with speeds S_1 for the applicator roll bringing in the liquid and S_2 for the backing roll supporting the web; the flow divides to form films of thickness d_1 and d_2 (Figure 2). At low capillary number, the same meniscus radius of curvature, R, is imposed on both films in the Landau-Levich Equation 3, and it follows that the flow splits according to $d_2/d_1 = (S_2/S_1)^{2n/(1+2n)}$. This result agrees with Gaskell et al.'s (1998b) experimental results in the Newtonian case. With the nip flooded upstream (i.e., the flow rate supplied greatly exceeds that through the nip), the film-forming meniscus remains downstream of the nip and the flow rate is approximately that for totally submerged rollers; this situation is therefore suited to metering flow. If metering is not the main objective and the feed to the nip is restricted, thinner films can be formed. An upstream meniscus appears, and a liquid bridge or bead spans the gap between the rollers (as shown in Figure 1*b* and Figure 2). As the speed of the backing roller S_2 increases with the speed of the applicator roller S_1 fixed (and hence the flow rate supplied), the upstream meniscus can pass through the nip and

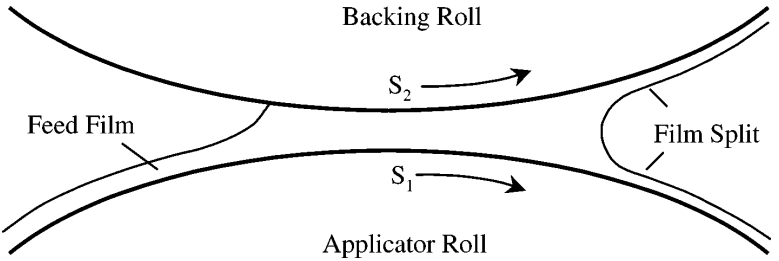

Figure 2 Enlarged schematic of the narrow channel region of Figure 1*b* in forward roll coating.

remain stable over a small range of speeds (Gaskell et al. 1998b). In this diverging channel, surface tension becomes destabilizing and the bead can break. Gaskell et al. (2001) modeled the steady state and its linear stability, finding a limit point of the steady solutions where the flow becomes unstable. Their predictions for the positions of the menisci and loss of stability agree with experimental measurements. Gaskell et al. (1998a) and Thompson et al. (2001) obtained similar results for reverse roll coating ($S_1 > 0$ and $S_2 < 0$).

Forward roll coating is prone to the classic ribbing instability in which the film thickness becomes spatially periodic transverse to the coating direction (see photographs by Soules et al. 1988). The instability arises because the positive pressure gradient in a channel with diverging walls is destabilizing (Savage 1992). Surface tension is stabilizing, so films formed at sufficiently small capillary number are uniform. The onset of ribbing can be predicted from a standard linear stability analysis (Coyle 1990, Carter & Savage 1987). Gurfinkel Castillo & Patera (1997) solved the full nonlinear equation set numerically for the steady ribbed state. Experiments show that as speed increases, the ribs become unsteady and ultimately spatter and spray occur (Adachi et al. 1988).

In blade coating (Figure 1*c*), a flexible blade is pressed against a backing roller with an elastomeric cover to control coat weight. The blade offers the advantage that a divergent channel and the associated ribbing instability can be avoided. Boundary conditions for the lubrication flow are straightforward because a single film forms at the blade tip. Bousfield et al. (1998) modeled blade coating and found that a softer cover increases the force on the blade needed to obtain the same coat weight. The cover forms a shoulder near the toe of the blade, and increasing deformation leads to no solution and the expectation of a resulting lower limit to coat weight.

Metering and film formation by narrow channels is substantially complicated if the web is porous, as is, for example, a paper web. A significant contribution to coat weight arises through the instantaneous filling of surface roughness and surface pores, evidenced by a minimum coat weight as blade loading is increased (Kuzmak 1986). Capillary pressure draws in liquid (Smiles 1998), and hydrodynamic pressure forces penetration (Windle & Beazley 1967, Clark et al. 1969, Salminen 1988). When a suspension of pigment is coated on paper, the suspending

liquid penetrates the paper (dewatering), but the pigment particles can remain on its surface as a filter cake. A filter cake of packed particles exhibits a much higher viscosity than the suspension and can be considered immobile. Bousfield (1994) modeled blade coating with filter-cake formation using Darcy's Law and found a minimum coat weight resulting from the filter cake that cannot be reduced without excessive blade pressure.

A significant unresolved problem of blade coating is the buildup of material behind the blade, and at the blade tip, as coating speed and solids content are increased. Excessive filter-cake growth (Bousfield 1994) may be responsible or colloidal instabilities and shear-induced aggregation (Roper & Attal 1993). As in roll coating, spatter and spray can occur and are exacerbated by a diverging channel when the blade runs on its heel.

PREMETERED FLOW ELEMENTS

Coating Die

In premetered coating processes, coating dies are used to form sheets or films of liquids in preparation for coating (Figure 1*c*,*d*,*e*). The performance of a die is assessed by the uniformity along the width of the liquid film (i.e., transverse to the coating direction), which the internal geometry determines. In typical designs, at least one cavity and an adjoining slot span the width of the die and distribute the liquid that is supplied to the center or end of the cavity (Figure 3). Kistler & Schweizer (1997) review die flows.

The operating principle of coating dies is the partitioning of pressure and is most easily understood for a single cavity die. Typically, the breadth of the cavity is large compared to the height of the slot; as a result, the resistance to flow is higher in the slot, and the liquid is thus distributed along the width. The shear rate in the cavity is lower than that in the slot. For the purpose of estimating for a shear-thinning liquid, we may therefore treat the liquid as being Newtonian in the

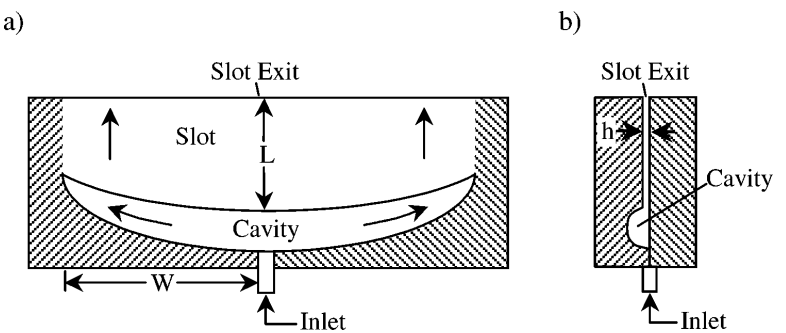

Figure 3 Single cavity die geometry. (*a*) Plan view; (*b*) side view. The arrows in the cavity and slot denote the predominant flow directions.

cavity and slot with apparent viscosities denoted by μ_c and μ_s, respectively. Die flows are viscous dominated, and the order of magnitude of the pressure drop along the cavity, ΔP_c, and the slot, ΔP_s, follows from Poiseuille flow in each region. We obtain the ratio

$$\frac{\Delta P_c}{\Delta P_s} \propto \left(\frac{\mu_c}{\mu_s}\right)\left(\frac{W^2 h^3}{L A^2}\right), \tag{8}$$

where W is the distance from the inlet to the end of the die (the die has width $2W$), h is the slot height, L is a characteristic slot length, and A is a characteristic cross-sectional area of the cavity (Figure 3). Performance improves as the ratio $\Delta P_c/\Delta P_s$ in Equation 8 decreases, and the cavity approaches a constant pressure reservoir. The second bracketed term in Equation 8 indicates the efficacy of small slot height and large cavity area. Additionally, in the absence of inlet effects associated with inertia (Wen et al. 1994), center-fed dies perform better than end-fed dies (Carley 1954) for the same coating width because W is half as large (Figure 3). Equation 8 also shows that shear thinning degrades performance by increasing the ratio μ_c/μ_s (see, for example, Carley 1954, Leonard 1985a, Liu et al. 1988). Inertia gives rise to recovered pressure at the cavity ends that reduces the pressure drop ΔP_c from that given by Equation 8, and this favorable effect can be significant for low-viscosity liquids and high flow rates (Leonard 1985a).

Die geometry is altered to enhance performance (Figure 3). For example, a decrease in the slot length with widthwise location (Figure 3*a*) partly compensates for the pressure drop along the cavity. The specification of the slot length taper is an optimization because the pressure drops depend on rheology and flow rate. A progressive reduction of cavity area in the flow direction (Figure 3*a*) reduces stagnation at the ends. Reduced cavity area degrades performance as shown in Equation 8, and this drawback must be balanced against the benefits of streamlining. A second cavity and slot (see Figure 1*e*) enhances uniformity and versatility (Leonard 1985b, Lee & Liu 1989, Ruschak & Weinstein 1997a). Additionally, mechanical (Kistler & Schweizer 1997, Ruschak & Weinstein 1997b) and pressure-induced tolerances (Pearson 1964, Sander & Pitman 1996, Gifford 1998) greatly influence die design. Design is an optimization based on objectives.

The flow in dies is modeled by solving simplified equations or complete equations in three dimensions. The unsimplified approach (Nguyen & Kamal 1990, Wen et al. 1994) is computationally intensive because of the nonlinear equations and the graded meshes required by the disparate dimensions in the die. In the simplified approach, the cavity aspect ratio is assumed to satisfy $A^{1/2} \ll W$, and resulting three-dimensional equations are averaged across the cavity to obtain approximate nonlinear ordinary differential equations relating flow to pressure (Leonard 1985b, Weinstein & Ruschak 1996, Ruschak & Weinstein 1997a). However, there are incorrect forms of the cavity equations in the literature for both single- and two-cavity dies (Weinstein & Ruschak 1996, Ruschak & Weinstein 1997b). Because the predominant flow in the first cavity is widthwise (as indicated in Figure 3*a*), and that in a second cavity is in its cross section (towards

the slot exit), the equations for flow are different except for creeping flow. The simplified equations in the slot are one-dimensional when the slot length is much smaller than its width ($L \ll W$) (Weinstein & Ruschak 1996). However, two-dimensional slot equations, which utilize the Hele-Shaw approximation (Sartor 1990, Vrahapoulou 1991), are required when these dimensions are comparable ($L \sim W$). A two-dimensional analysis in the slot is also required in the vicinity of end walls that are angled (i.e., the slot width does not everywhere equal $2W$) to control edge effects (Friedman 1998). Dies having $L \sim W$ with slowly varying cavity shapes amenable to lubrication theory have been completely analyzed using two-dimensional analysis (Vergnes et al. 1984, Smith et al. 1998). Linearization about the limit of perfect distribution can facilitate solving the simplified equations (Durst et al. 1994, Weinstein & Ruschak 1996, Ruschak & Weinstein 1997a). A major advantage of the one-dimensional approach is the particularly simple posing and solving of an inverse problem in which the geometric parameters are explicitly calculated for a perfect flow distribution (Pearson 1964, Winter & Fritz 1986, Durst et al. 1994). A disadvantage is that flow details, such as recirculations (Lee & Liu 1989, Lee et al. 1990) and inlet entrance effects (Wen et al. 1994), cannot be predicted.

Slide Delivery

Liquid layers are stacked on the inclined surfaces of a die (Figure 1*d*,*e*) in preparation for simultaneous coating onto a web. Slide flows are driven by gravity and can amplify waves initiated by ambient perturbations that degrade the uniformity of a coating. These waves travel along each interface in the system, and the number of waves is equal to the number of interfaces across which a physical property, such as viscosity, density, or surface tension, changes (Figure 1*e*). Joseph & Renardy (1992) and Chen (1995) review the extensive literature on the stability of this flow.

Wave propagation can be examined through linear analysis, which leads to an exponential growth or decay of waves. Nonlinear dynamics of waves is the subject of much current research (Chang 1994, Pozrikidis 1998, Kliakhandler 1999) but may not have to be considered in coating applications when coated uniformity requirements are stringent. Tollmien-Schlichting-type wave instabilities (Floryan et al. 1987, Woods & Lin 1996) are usually outside the range of interest as well.

Although much literature addresses the neutral stability of inclined plane flows, the issue of most importance in coating is the degree of wave growth or decay that occurs. The case of long wavelengths has been extensively analyzed (Yih 1963, Kao 1968, Wang et al. 1978), but intermediate wavelengths often exhibit larger growth (Loewenherz & Lawrence 1989, Kobayashi 1992, Weinstein & Chen 1999). In fact, waves stable at long wavelengths may be unstable at intermediate ones (Chen 1993). A comparison of stability predictions for Newtonian and shear-thinning cases indicates that shear thinning does not give rise to additional instability mechanisms, but the rate of growth and decay can be significantly affected (Weinstein 1990).

The instabilities are convective (Brevdo et al. 1999) and usually arise from ambient perturbations to the flow that are often temporally periodic (e.g., flow perturbations caused by vibrations, pumps, and fans). Such waves grow spatially (Krantz & Owens 1973, Pierson & Whitaker 1977, Weinstein 1990, Kobayashi 1992), and temporal growth occurs only under transient conditions. Temporal and spatial growth may not be related via Gaster's transformation (Gaster 1962) because growth or decay typically occurs far from neutral stability. The convective nature of the instability ensures that the amplitude of spatially growing waves is bounded at any location. Therefore, the waves are advantageously viewed in the context of a wavemaker problem (Weinstein et al. 1993), in which initial perturbations combine with wave evolution to yield the amplitude at the end of the incline. In this regard, even if flow is stable, a large disturbance can lead to a nonuniform coating. Slide waves in coatings typically show nearly parallel wave fronts extending widthwise, and thus two-dimensional analysis is adequate.

Liquid Curtain

Freely falling liquid sheets, called curtains, are formed from dies or weirs and impinge on the web (Figure 1*e*). Curtains are essentially the planar analogue of water bells (Finnicum et al. 1993). At the top of the curtain, the velocity field adapts to the loss of viscous traction with the die. When formed from a die having a slide (Figure 1*e*), there is no vertical plane of symmetry, and this flow rearrangement can result in pronounced deflection of the curtain towards the die (Kistler & Scriven 1994). This entry region for the curtain provides boundary conditions that are applied to simplified equations based on the asymptotics of a gradually thinning sheet that can accurately predict steady and transient flows. The undisturbed flow in a freely falling curtain can be described with the semiempirical equation of Brown (1961), whose form is consistent with Taylor's asymptotically correct equation (Clarke 1968, Ramos 1996) at high Reynolds numbers (Weinstein et al. 1997). Under such circumstances, the flow may be considered inviscid (Finnicum et al. 1993, Weinstein et al. 1997, Clarke et al. 1997). In multiple-layer applications of similar density liquids, the inviscid approximation allows the flow to be examined as for a single layer.

If ruptured, a curtain spontaneously reforms if the Weber number, $We = \rho q V/2\sigma$ (V is the local velocity of the curtain), exceeds unity everywhere. Conversely, if a free edge or hole occurs where $We < 1$, the curtain disintegrates into a series of vertical liquid threads (Pritchard 1986). Practically, it is necessary for $We > 1$ at the impingement point of the curtain to avoid air entrainment at low speeds, make starts and stops, and maintain contact with the edge guides used to maintain curtain width against surface tension. The sensitivity of a stable curtain to ambient perturbations is of importance when coating uniformity requirements are stringent. Pressure fluctuations on the curtain due to air flow induce propagating waves (Lin 1981, Weinstein et al. 1997, Clarke et al. 1997) that distort the curtain and degrade coating uniformity. Even in the absence of time-dependent

perturbations, the curtain shape may be distorted by stationary waves (Lin & Roberts 1981, De Luca & Costa 1997, Weinstein et al. 1998). Stationary waves arise at the die lip and edge guides and can lead to streaks in the coating (Kistler & Schweizer 1997).

Small Gap

In slot and slide and other coating methods (Kistler & Schweizer 1997), a liquid bridge, often called a bead, spans a gap of order 100 microns between the web and another solid boundary (Figure 1*c*,*d*). At low *Ca*, the operating range of slot coating follows from the possible configurations of the essentially static interfaces of constant curvature that bound the bead (Ruschak 1976, Higgins & Scriven 1980). The radius of the downstream film-forming meniscus follows from coating thickness, web speed, and liquid properties through the Landau-Levich Equation 3. The upstream radius follows from the dynamic contact angle and the pressure drop imposed across the bead (suction assist, Figure 1*d*). Failure occurs when either radius is too small to span the gap. The failure of the upstream interface limits the range of suction assist, and that of the downstream interface limits coating speed and thickness (in the absence of air entrainment). These considerations are valid for slide coating as well, but the downstream meniscus is constrained by tangency to the slide. As a consequence of this constraint, the minimum radius in slide coating is larger than that in slot coating, and therefore slide coating is limited to thicker coatings for the same gap. At somewhat larger values of *Ca* and *Re*, the Landau-Levich result may be replaced with the solution to a film equation incorporating inertia (Carvalho & Kheshgi 2000) and, apart from this, the operating range is deduced geometrically as at low *Ca*.

A consequence of the Landau-Levich Equation 3 is that the minimum possible film thickness increases with increasing *Ca* in a fixed geometry. In slot coating at high *Ca* and *Re*, this trend reverses (Carvalho & Kheshgi 2000) and allows for thinner coatings with increasing speed. Carvalho & Kheshgi postulate that this change occurs due to a Sakiadis boundary layer that couples the upstream and downstream interfaces of the bead. Possible support for this proposal comes from experiments in which changes to suction affect the radius of curvature of the downstream meniscus (Hens & Boiy 1986), whereas suction has no effect at low *Ca*. The effect of inertia requires more experimental and theoretical investigation.

FLOW AFTER COATING

Coatings continue to flow after application in response to perturbations until immobilized by gelling, curing, dewatering, or drying (Quach 1973, Kornum & Raaschou Nielson 1980, Kistler & Schweizer 1997). Impinging air flows can distort interfaces and can cause flow (Ruschak 1987). Temperature variations along the air-liquid interface may result from rapid evaporation and nonisothermal contact with

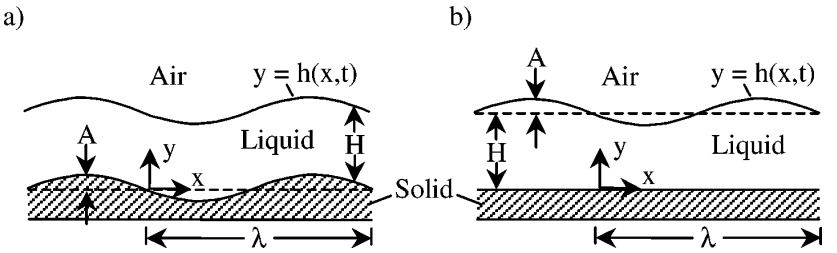

Figure 4 Schematic showing initial interface deformation leading to flow after coating. (*a*) Uniform film on an uneven web; (*b*) nonuniform film on a flat web.

convecting air and with conveyance hardware (Wilson 1997, Howison et al. 1997), giving rise to surface tension-driven flow. Impinging air may deposit surface-active contaminants on the coating and, in some cases, chemical components or contaminants of the coating may be surface active. The resulting reduction in surface tension can cause craters or holes (also called repellencies) in the coating (Kheshgi & Scriven 1991).

If a horizontal web is uneven but initially coated conformally (Figure 4*a*), or a flat horizontal web is not coated uniformly (Figure 4*b*), flow after coating occurs due to surface tension and gravity. Both situations may be treated as a superposition of Fourier cosine components of wavelength λ and amplitude A (Figure 4) and if $A \ll H$, where H is the mean thickness of the film, the analyses are identical (Joos 1996). Using the coordinate system shown in Figure 4 and denoting t as time, the location of the interface, $y = h(x, t)$, follows from lubrication theory for $H \ll \lambda$:

$$h = H + A\exp\left[-\frac{H^3(2\pi)^2}{3\mu\lambda^2}\left(\frac{\sigma(2\pi)^2}{\lambda^2} \pm \rho g\right)t\right]\cos\left(\frac{2\pi}{\lambda}x\right). \qquad (9)$$

Here, the plus sign is taken when the coating faces upward and the minus sign is taken when it faces downward. Leveling of the interface always occurs with the coating facing upward, but it occurs only at small wavelengths with the coating facing downward. For an uneven web, A is the amplitude of the unevenness, and the fractional thickness variation in the film, f, is given by $f = [h\text{-}H\text{-}A\ cos(2\pi x/\lambda)]/H$; a leveled interface, i.e., $h = H$ in Equation 9, gives a film of nonuniform thickness. For a flat web and an initially nonuniform film thickness of amplitude A, the fractional thickness variation is $f = (h\text{-}H)/H$, and a leveled interface gives a film of uniform thickness. Thus, leveling the interface can improve or degrade coating uniformity.

Surfactants give rise to surface-tension gradients, tending to oppose the flow of the film (Schwartz et al. 1995). However, variations in surfactant concentration arise through flow induced by surface tension and gravity, and so surface-tension gradients are delayed (Joos 1996) and may follow after leveling of the air-liquid interface. At wavelengths on the order of film thickness, leveling rates are reduced

(Orchard 1962) from those given by Equation 9, as evident for the extreme case $\lambda \ll H$, where the velocity component tangent to the interface becomes zero as a result of strong coupling between velocity components. Three-dimensional analysis yields a leveling equation similar to that for the two-dimensional case (Anshus 1973). Inertia can lead to oscillations during leveling (Kheshgi 1989). Shear thinning promotes leveling by reducing the effective viscosity of the film (Iyer & Bousfield 1996). Leveling of films is retarded by absorption into a porous web, which reduces the film thickness and can immobilize the film (Bousfield 1991). For multiple-layer coatings of miscible liquids with substantially equal densities, flow is driven by the air-liquid interface as for a single layer. However, the internal interfaces do not necessarily level even in an upright configuration; the flow ends when the air-liquid interface is essentially flat and surface tension gradients are dissipated (Joos 1996).

Coatings also flow along inclined webs by gravity. In a frame of reference stationary with respect to the web, the previously addressed configuration of flow down an inclined plane is recovered, and waves can arise. However, as the coated film thickness is much smaller on the web than on the slide, the flow rate in the web frame of reference is so small that inertial effects, which tend to promote wave growth, are small (Weinstein & Chen 1999). Nevertheless, in coatings of three or more layers on a flat web in certain viscosity configurations, strong instabilities can arise even in the absence of inertia and produce significant deformations of the interior interfaces (Weinstein & Chen 1999). Beyond the issue of stability, flow on inclines can produce wakes around inclusions carried with the flow or arrested on the web (Pozrikidis & Thoroddsen 1991).

CLOSING COMMENTS

Coating processes are complex and have been largely developed empirically together with an informal and often nonscientific conceptual framework. Scientific approaches are increasingly important in their refinement and efficient application as the transformation from coating art to science continues. Physical insights provide valuable guidance of experimentation, even when predictive models are not possible or when the parameters of the models are difficult, costly, or impossible to measure. Complex coating processes can be designed and modeled by combining flow elements that are empirically or analytically understood.

ACKNOWLEDGMENTS

We would like to thank our main colleagues at Eastman Kodak Company, notably F. Miguel Joos, Marc Bermel, Andrew Clarke, Jean-Marie Baumlin, and Terry Blake, who have advanced our knowledge of coating. We would also like to thank Professor Paul Steen of Cornell University for many helpful discussions, and Eastman Kodak Company for supporting our work.

The *Annual Review of Fluid Mechanics* is online at http://fluid.annualreviews.org

LITERATURE CITED

Adachi K, Tamura T, Nakamura R. 1988. Coating flows in a nip region and various critical phenomena. *AIChE J.* 34(3):456–64

Andersson HI. 1987. The momentum integral approach to laminar thin-film flow. *Proc. ASME Symp. Thin Films* 48:7–13

Anshus BE. 1973. The leveling process in polymer powder painting—A three dimensional approach. *Chem. Soc. Div. Org. Coat. Plast. Chem.* 33(2):493–501

Benkreira H, Cohu O. 1998. Angling the wetting line retards air entrainment in premetered coating flows. *AIChE J.* 44(5):1207–9

Blake TD, Bracke M, Shikhmurzaev YD. 1999. Experimental evidence of nonlocal hydrodynamic influence on the dynamic contact angle. *Phys. Fluid.* 11(8):1995–2007

Blake TD, Clarke A, Ruschak KJ. 1994. Hydrodynamic assist of dynamic wetting. *AIChE J.* 40(2):229–42

Blake TD, De Coninck J. 2002. The influence of solid-liquid interactions on dynamic wetting. *Adv. Colloid Interface Sci.* 96:21–36

Blake TD, Shikhmurzaev YD. 2002. Dynamic wetting by liquids of different viscosity. *J. Colloid Interface Sci.* 253:196–202

Bohr T, Putkaradze V, Watanabe S. 1997. Averaging theory for the structure of hydraulic jumps and separation in laminar free-surface flows. *Phys. Rev. Lett.* 79:1038–41

Bousfield DW. 1991. A model to predict the leveling of coating defects. *Tappi J.* 74(5):163–70

Bousfield DW. 1994. Prediction of velocity and coat-weight limits based on filter-cake formation. *Tappi J.* 77(7):161–71

Bousfield DW, Rigdahl M, Wikstrom M. 1998. Roll deformation during blade coating. *Tappi J.* 81(5):207–12

Brevdo L, Laure P, Dias F, Bridges TJ. 1999. Linear pulse structure and signalling in a film flow on an inclined plane. *J. Fluid Mech.* 396:37–71

Brown DR. 1961. A study of the behaviour of a thin sheet of moving liquid. *J. Fluid Mech.* 10:297–305

Cameron A. 1976. *Basic Lubrication Theory*. New York: Wiley

Carley JF. 1954. Flow of melts in "crosshead"-slit dies; criteria for die design. *J. Appl. Phys.* 25(9):1118–23

Carter GC, Savage MD. 1987. Ribbing in a variable speed two-roll coater. *Math. Eng. Ind.* 1(1):83–95

Carvalho MS, Kheshgi HS. 2000. Low-flow limit in slot coating: theory and experiments. *AIChE J.* 46(10):1907–17

Carvalho MS, Scriven LE. 1997. Flows in forward deformable roll coating gaps: comparison between spring and plane-strain models of roll cover. *J. Comp. Phys.* 138:449–79

Cerro RL, Scriven LE. 1980. Rapid free surface film flows: An integral approach. *Ind. Eng. Chem. Fundam.* 19:40–50

Chang HC. 1994. Wave evolution on a falling film. *Annu. Rev. Fluid Mech.* 26:103–36

Chen KP. 1993. Wave formation in the gravity-driven low-Reynolds number flow of two liquid films down an inclined plane. *Phys. Fluid.* 5(12):3038–48

Chen KP. 1995. Interfacial instabilities in stratified shear flows. *Appl. Mech. Rev.* 48(11):763–76

Clark NO, Windle W, Beazley KM. 1969. Liquid migration in blade coating. *Tappi J.* 52(11):2191–202

Clarke A. 2002. Coating on a rough surface. *AIChE J.* 48(10):2149–56

Clarke A, Weinstein SJ, Moon AG, Simister EA. 1997. Time-dependent equations governing the shape of a two-dimensional liquid curtain, Part II: Experiment. *Phys. Fluid.* 9(12):3637–44

Clarke NS. 1968. Two-dimensional flow under gravity in a jet of viscous liquid. *J. Fluid Mech.* 31:481–500

Cohu O, Benkreira H. 1998a. Air entrainment in angled dip coating. *Chem. Eng. Sci.* 53(3):533–40

Cohu O, Benkreira H. 1998b. Entrainment of air by a solid surface plunging into a non-Newtonian liquid. *AIChE J.* 44(11):2360–68

Cohu O, Magin A. 1997. Forward roll coating of Newtonian fluids with deformable rolls: an experimental investigation. *Chem. Eng. Sci.* 52:1339–47

Cox RG. 1998. Inertial and viscous effects on dynamic contact angles. *J. Fluid Mech.* 357:249–78

Coyle DJ, Macosko CW, Scriven LE. 1990. Stability of symmetric film-splitting between counter-rotating cylinders. *J. Fluid Mech.* 216:437–58

Coyle DJ, Macosko CW, Scriven LE. 1986. Film-splitting flows in forward roll coating. *J. Fluid Mech.* 171:183–207

De Luca L, Costa M. 1997. Stationary waves on plane liquid sheets falling vertically. *Eur. J. Mech. B/Fluid.* 16(1):75–88

de Ruijter MJ, Blake TD, De Coninck J. 1999. Dynamic wetting studied by molecular modeling simulations of droplet spreading. *Langmuir* 15:7836–47

Deryagin BM, Levi SM. 1964. *Film Coating Theory.* New York: Focal Press

Dowson D, Higginson GR. 1977. *Elasto-Hydrodynamic Lubrication*. Oxford: Pergamon, 2nd Ed.

Dressler RF. 1949. Mathematical solution of the problem of roll waves in inclined open channels. *Commun. Pure Appl. Math.* 2:149–94

Durst F, Lange U, Raszillier H. 1994. Optimization of distribution chambers of coating facilities. *Chem. Eng. Sci.* 49(2):161–70

Dutta A, Mashelkar RA. 1982. On slip effect in free coating of non-Newtonian fluids. *Rheol. Acta.* 21:52–61

Finnicum DS, Weinstein SJ, Ruschak KJ. 1993. The effect of applied pressure on the shape of a two-dimensional liquid curtain falling under the influence of gravity. *J. Fluid Mech.* 255:647–65

Floryan JM, Davis SH, Kelly RE. 1987. Instabilities of a liquid film flowing down an inclined plane. *Phys. Fluid.* 30(4):983–89

Fox VG, Erickson LE, Fan LT. 1969. The laminar boundary layer on a moving continuous flat sheet immersed in a non-Newtonian fluid. *AIChE J.* 15(3):327–33

Friedman A. 1998. *Mathematics in Industrial Problems*, pp. 50–61. New York: Springer

Gaskell PH, Innes GE, Savage MD. 1998b. An experimental investigation of meniscus roll coating. *J. Fluid Mech.* 355:17–44

Gaskell PH, Kapur N, Savage MD. 2001. Bead-break instability. *Phys. Fluid.* 13(5):1243–53

Gaskell PH, Savage MD, Thompson HM. 1998a. Stagnation-saddle points and flow patterns in Stokes flow between contra-rotating cylinders. *J. Fluid Mech.* 370:221–47

Gaster M. 1962. A note on the relation between temporally-increasing and spatially increasing disturbances in hydrodynamic stability. *J. Fluid Mech.* 14:222–24

Ghannam MT, Esmail MN. 1997. Experimental study on wetting of fibers with non-Newtonian liquids. *AIChE J.* 43(6):1579–88

Gifford WA. 1998. A three-dimensional analysis of the effect of die body deflection in the design of extrusion dies. *Polym. Eng. Sci.* 38(10):1729–39

Groenveld P. 1970. High capillary number withdrawal from viscous Newtonian liquids by flat plates. *Chem. Eng. Sci.* 25:33–40

Gutfinger C, Tallmadge J. 1965. Films of non-Newtonian fluids adhering to flat plates. *AIChE J.* 11(3):403–13

Gurfinkel Castillo ME, Patera AT. 1997. Three-dimensional ribbing instability in symmetric forward-roll film-coating processes. *J. Fluid Mech.* 335:323–59

Halpern D, Jensen OE. 2002. A semi-infinite bubble advancing into a planar tapered channel. *Phys. Fluid.* 14(2):431–42

Hansen RJ, Toong TY. 1971. Dynamic contact angle and its relationship to forces of hydrodynamic origin. *J. Colloid Interface Sci.* 37(1):196–207

Hens J, Boiy L. 1986. Operation of the bead of a pre-metered coating device. *Chem. Eng. Sci.* 41(7):1827–31

Higgins BG, Scriven LE. 1980. Capillary pressure and viscous pressure drop set bounds on coating bead operability. *Chem. Eng. Sci.* 35:673–82

Hildebrand RE, Tallmadge JA. 1968. A test of the withdrawal theory for Ellis fluids. *Can. J. Chem. Eng.* 46:394–97

Howison SD, Moriarty JA, Ockendon JR, Terrill EL, Wilson SK. 1997. A mathematical model for drying paint layers. *J. Eng. Math.* 32:377–94

Iyer RR, Bousfield DW. 1996. The leveling of coating defects with shear-thinning rheology. *Chem. Eng. Sci.* 51(20):4611–17

Joos FM. 1996. Leveling of a film with stratified viscosity and insoluble surfactant. *AIChE J.* 42(3):623–37

Joseph DD, Renardy Y. 1992. *Fundamentals of Two Fluid Dynamics*. New York: Springer-Verlag

Kao TW. 1968. Role of viscosity stratification in the stability of two-layer flow down an incline. *J. Fluid Mech.* 33:561–72

Kheshgi HS. 1989. Profile equations for film flows at moderate Reynolds numbers. *AIChE J.* 35:(10)1719–27

Kheshgi HS, Kistler SF, Scriven LE. 1992. Rising and falling film flows: viewed from a first-order approximation. *Chem. Eng. Sci.* 47:683–94

Kheshgi HS, Scriven LE. 1991. Dewetting: nucleation and growth of dry regions. *Chem. Eng. Sci.* 46(2):519–26

Kistler SF, Schweizer PM, eds. 1997. *Liquid Film Coating*. London: Chapman & Hall

Kistler SF, Scriven LE. 1994. The teapot effect: Sheet-forming flows with deflection, wetting and hysteresis. *J. Fluid Mech.* 263:19–62

Kitzio JP, Kamotani Y, Ostrach S. 1999. Experimental free coating flows at high capillary and Reynolds number. *Exp. Fluid.* 27:235–43

Kliakhandler IL. 1999. Long interfacial waves in multilayer thin films and coupled Kuramoto-Sivashinsky equations. *J. Fluid Mech.* 391:45–65

Kobayashi C. 1992. Stability analysis of film flow on an inclined plane I. One layer, two layer flow. *Ind. Coating Res.* 2:65–88

Kornum LO, Raaschou Nielson HKR. 1980. Surface defects in drying paint films. *Prog. Org. Coatings* 8:275–324

Krantz WB, Owens WB. 1973. Spatial formulation of the Orr-Sommerfeld equation for thin liquid films flowing down a plane. *AIChE J.* 19(6):1163–69

Kuzmak JM. 1986. Bevelled-blade coating. *Tappi J.* 69(2):72–75

Lee KY, Liu TJ. 1989. Design and analysis of a dual-cavity coat-hanger die. *Polym. Eng. Sci.* 29(15):1066–75

Lee KY, Wen SH, Liu TJ. 1990. Vortex formation in a dual-cavity coat hanger die. *Polym. Eng. Sci.* 30(19):1220–27

Lehtinen E, ed. 2000. *Pigment Coating and Surface Sizing of Paper*. Helskinki, Finland: Gummerus Printing

Leonard WK. 1985a. Inertia and gravitational effects in extrusion dies for non-Newtonian fluids. *Polym. Eng. Sci.* 25(9):570–76

Leonard WK. 1985b. Effects of secondary cavities, inertia, and gravity on extrusion dies. *SPE ANTEC Tech. Papers* 31:144–48

Levich VG. 1962. *Physiochemical Hydrodynamics*. Englewoood Cliffs/New Jersey: Prentice-Hall

Lin SP. 1981. Stability of a viscous liquid curtain. *J. Fluid Mech.* 104:111–118

Lin SP, Roberts G. 1981. Waves in a viscous liquid curtain. *J. Fluid Mech.* 112:443–58

Liu TJ, Hong CN, Chen KC. 1988. Computer aided analysis of a linearly tapered coat-hanger die. *Polym. Eng. Sci.* 28(23):1517–26

Loewenherz DS, Lawrence CJ. 1989. The effect of viscosity stratification on the stability of a free surface flow at low Reynolds number. *Phys. Fluid.* 1(10):1686–93

Nguyen KT, Kamal MR. 1990. Blow molding die design for non-axisymmetric parison extrusion. *Polym. Eng. Sci.* 30(23):1537–43

Orchard SE. 1962. On surface levelling in viscous liquids and gels. *Appl. Sci. Res. A.* 11:451–64

Pearson JRA. 1964. Non-Newtonian flow and die design. *Trans. J. Plast. Inst.* 32:239–44

Petrov JG, Sedev RV. 1985. On the existence of a maximum speed of wetting. *Colloids Surf.* 13:313–22

Pierson FW, Whitaker S. 1977. Some theoretical and experimental observations of the wave structure of falling liquid films. *Ind. Eng. Chem. Fundam.* 16(4):401–8

Pozrikidis C. 1998. Gravity-driven creeping flow of two adjacent layers through a channel and down a plane wall. *J. Fluid Mech.* 371:345–76

Pozrikidis C, Thoroddsen ST. 1991. The deformation of a liquid film flowing down an inclined plane wall over a small particle arrested on the wall. *Phys. Fluid.* 3(11):2546–58

Pritchard WG. 1986. Instability and chaotic behaviour in a free-surface flow. *J. Fluid Mech.* 165:1–60

Quach A. 1973. Polymer coatings. Physics and mechanics of leveling. *Ind. Eng. Chem. Prod. Res. Dev.* 12(2):110–16

Ramos JI. 1996. Planar liquid sheets at low Reynolds number. *Int. J. Num. Meth. Fluid.* 22:961–78

Reglat O, Labrie R, Tanguy PA. 1993. A new free surface model for the dip coating process. *J. Comp. Phys.* 109:238–246

Roper III JA, Attal JF. 1993. Evaluations of coating high-speed runnability using pilot coater data, rheological measurements, and computer modeling. *Tappi J.* 76(5):55–61

Rosenhead L. 1940. The steady two-dimensional radial flow of viscous fluid between two inclined plane walls. *Proc. R. Soc. London* 175:436–67

Ruschak KJ. 1982. Boundary conditions at a liquid/air interface in lubrication flows. *J. Fluid Mech.* 119:107–20

Ruschak KJ. 1974. *The Fluid Mechanics of Coating Flows*. PhD thesis. Univ. Minn., Minneapolis

Ruschak KJ. 1976. Limiting flow in a premetered coating device. *Chem. Eng. Sci.* 31:1057–60

Ruschak KJ. 1978. Flow of a falling film into a pool. *AIChE J.* 24(4):705–9

Ruschak KJ. 1985. Coating flows. *Annu. Rev. Fluid Mech.* 17:65–89

Ruschak KJ. 1987. Flow of a thin liquid layer due to ambient disturbances. *AIChE J.* 33(5):801–7

Ruschak KJ. 1991. Technical note on forward roll coating. *Ind. Coating Res.* 1:59–62

Ruschak KJ, Weinstein SJ. 1997a. Perturbation solution for flow in two-cavity dies. *ASME J. Fluid. Eng.* 119:1003–8

Ruschak KJ, Weinstein SJ. 1997b. Modeling the secondary cavity of two-cavity dies. *Polym. Eng. Sci.* 35(12):1970–76

Ruschak KJ, Weinstein SJ. 1999. Viscous thin-film flow over a round-crested weir. ASME *J. Fluid. Eng.* 121:673–77

Ruschak KJ, Weinstein SJ, Ng K. 2001. Developing film flow on an inclined plane with a critical point. *ASME J. Fluid. Eng.* 123:698–702

Ruschak KJ, Weinstein SJ. 2003. Laminar, gravitationally driven flow of a thin film on a curved wall. *ASME J. Fluid. Eng.* 125:10–17

Sakiadis BC. 1961a. Boundary-layer behavior on continuous solid surfaces I. Boundary-layer equations for two-dimensional and axisymmetric flow. *AIChE J.* 7(1):26–28

Sakiadis BC. 1961b. Boundary-layer behavior on continuous solid surfaces II. The boundary-layer on a continuous flat surface. *AIChE J.* 7(2):221–25

Salminen PJ. 1988. Water transport into paper—the effect of some liquid and paper variables. *Tappi J.* 71(9):195–200

Sander R, Pittman JFT. 1996. Simulation of slit dies in operation including the interaction between melt pressure and die deflection. *Polym. Eng. Sci.* 36(15):1972–89

Sartor L. 1990. *Slot Coating: Fluid Mechanics and Die Design*. PhD thesis. Univ. Minn., Minneapolis

Savage MD. 1992. Meniscus instability and ribbing. *Ind. Coating Res.* 2:47–58

Schlichting H. 1979. *Boundary Layer Theory*. New York: McGraw-Hill, 7th Ed.

Schwartz LW, Weidner DE, Eley RR. 1995. An analysis of the effect of surfactant on the

leveling behavior of a thin liquid coating layer. *Langmuir* 11:3690–93

Shen C, Ruth DW. 1998. Experimental and numerical investigations of the interface profile close to a moving contact line. *Phys. Fluid.* 10(4):789–99

Shikhmurzaev YD. 1997. Moving contact lines in liquid/liquid/solid systems. *J. Fluid Mech.* 334:211–49

Shikhmurzaev YD. 1996. Dynamic contact angles and flow in vicinity of moving contact lines. *AIChE J.* 42(3):601–12

Simpkins PG, Kuck VJ. 2000. Air entrapment in coatings by way of a tip streaming meniscus. *Nature* 403:641–43

Smiles DE. 1998. Water flow in filter paper and capillary suction time. *Chem. Eng. Sci.* 53(12):2211–18

Smith DE, Tortorelli DA, Tucker CL. 1998. Optimal design for polymer extrusion. Part I: Sensitivity analysis for nonlinear steady-state systems. *Comput. Methods Appl. Mech. Eng.* 167:283–302

Soules DA, Fernando RH, Glass JE. 1988. Dynamic uniaxial extensional viscosity (DUEV) effects in roll application I. Rib and web growth in commercial coatings. *J. Rheol.* 32:181–98

Spiers RP, Subbaraman CV, Wilkinson WL. 1975. Free coating of non-Newtonian liquids onto a vertical surface. *Chem. Eng. Sci.* 30:379–95

Thompson HM, Kapur N, Gaskell PH, Summers JL, Abbott SJ. 2001. A theoretical and experimental investigation of reservoir-fed, rigid-roll coating. *Chem. Eng. Sci.* 56:4627–41

Tsou FK, Sparrow EM, Goldstein RJ. 1967. Flow and heat transfer in the boundary layer on a continuous moving surface. *Int. J. Heat Mass Transfer.* 10:219–35

Tsou FK, Sparrow EM, Kurtz EF. 1966. Hydrodynamic stability of the boundary layer on a continuous moving surface. *J. Fluid Mech.* 26:145–61

Van Rossum JJ. 1958. Viscous lifting and drainage of liquids. *Appl. Sci. Res. A.* 7:121–44

Vergnes B, Saillard P, Agassant JF. 1984. Non-isothermal flow of a molten polymer in a coat-hanger die. *Polym. Eng. Sci.* 24(12): 980–87

Voinov OV. 1994. Closure of the hydrodynamic theory of wetting in a small scale region. *J. Appl. Mech. Tech. Phys.* 35(1):1–12

Vrahopoulou EP. 1991. A model for fluid flow in dies. *Chem. Eng. Sci.* 46(2):629–36

Walter JC, ed. 1993. *The Coating Processes.* Atlanta: Tappi Press

Wang CK, Seaborg JJ, Lin SP. 1978. Instability of multi-layered liquid films. *Phys. Fluid.* 21(10):1669–173

Watson EJ. 1964. The radial spread of a liquid jet over a horizontal plane. *J. Fluid Mech.* 20:81–99

Weinstein SJ. 1990. Wave propagation in the flow of shear-thinning fluids down an incline. *AIChE J.* 36(12):1873–89

Weinstein SJ, Baumlin JM, Servant J. 1993. The propagation of surface waves in flow down an oscillating inclined plane. *AIChE J.* 39(7):1113–23

Weinstein SJ, Chen KP. 1999. Large growth rate instabilities in three-layer flow down an incline in the limit of zero Reynolds number. *Phys. Fluid.* 11(11):3270–82

Weinstein SJ, Clarke A, Moon A, Simister EA. 1997. Time-dependent equations governing the shape of a two-dimensional liquid curtain, Part 1: Theory. *Phys. Fluid.* 9(12):3625–36

Weinstein SJ, Hoff JW, Ross DS. 1998. Time dependent equations governing the shape of a three-dimensional liquid curtain. *Phys. Fluid.* 10(8):1815–18

Weinstein SJ, Ruschak KJ. 1996. One-dimensional equations governing single-cavity die design. *AIChE J.* 42(9):2401–14

Weinstein SJ, Ruschak KJ. 1999. On the mathematical structure of thin film equations containing a critical point. *Chem. Eng. Sci.* 54(8):977–85

Weinstein SJ, Ruschak KJ. 2001. Dip coating on a planar non-vertical substrate in the limit of negligible surface tension. *Chem. Eng. Sci.* 56:4957–69

Wen SH, Liu TJ, Tsou JD. 1994. Three-dimensional finite element analysis of polymeric fluid flow in an extrusion die. Part 1: Entrance effect. *Polym. Eng. Sci.* 34(10): 827–34

Wilson MCT, Summers JL, Shikhmurzaev YD. 1999. Hydrodynamic assist of wetting: theoretical results. In *Proceedings of the 3rd European Coating Symposium 1999: Advances in Coating and Drying of Thin Films*, ed. F Durst, H. Raszillier, pp. 75–80. Germany: Shaker Verlag

Wilson SDR. 1982. The drag-out problem in film coating theory. *J. Eng. Math.* 16:209–21

Wilson SK. 1997. The deviation and analysis of a model of the drying process of a paint film. *Surf. Coatings Int.* 4:162–67

Windle W, Beazley KM. 1967. The mechanics of blade coating. *Tappi J.* 50(1):1–7

Winter HH, Fritz G. 1986. Design of dies for the extrusion of sheets and annular parisons: The distribution problem. *Polym. Eng. Sci.* 26(3):543–53

Woods DR, Lin SP. 1996. Critical angle of shear wave instability in a film. *J. Appl. Mech.* 63:1051–52

Yih CS. 1963. Stability of liquid flow down an inclined plane. *Phys. Fluid.* 6:321–30